

The Pentagon Integrals for Poncelet Families

Richard Evan Schwartz *

February 3, 2014

Abstract

The pentagram map is now known to be a discrete integrable system. We show that the integrals for the pentagram map are constant along Poncelet families. That is, if P_1 and P_2 are two polygons in the same Poncelet family, and f is a monodromy invariant for the pentagram map, then $f(P_1) = f(P_2)$. Our proof combines complex analysis with an analysis of the geometry of a degenerating sequence of Poncelet polygons.

1 Introduction

The *pentagram map* is a projectively natural map defined on the space of n -gons. The case $n = 5$ is classical; it goes back at least to Clebsch in the 19th century and perhaps even to Gauss. Motzkin [Mot] also considered this case in 1945. I introduced the general version of the pentagram map in 1991. See [Sch1]. I subsequently published two additional papers, [Sch2] and [Sch3], on the topic. Now there is a growing literature. See the discussion below.

To define the pentagram map, one starts with a polygon P and produces a new polygon $T(P)$, as shown at left in Figure 1.1 for a convex hexagon. As indicated at right, the map $P \rightarrow T^2(P)$ acts naturally on labeled polygons.

* Supported by N.S.F. Research Grant DMS-0072607 and also a Clay Research Scholarship

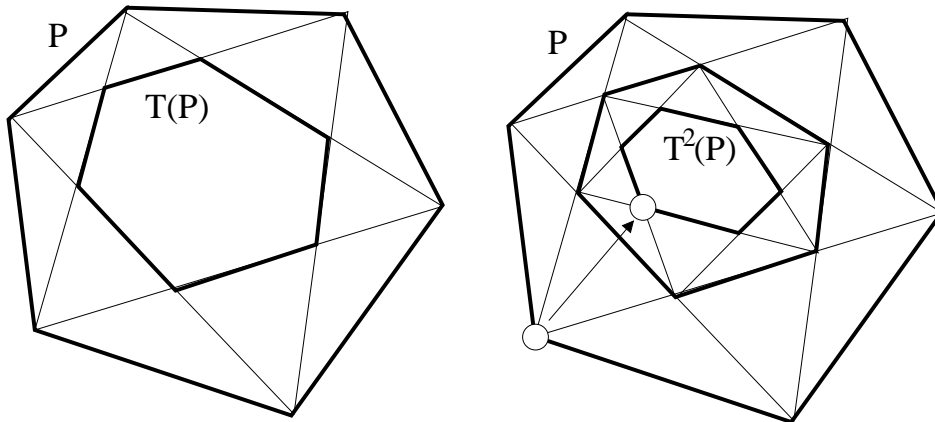


Figure 1.1: The pentagram map

The pentagram map is defined on polygons over any field. More generally, as I will discuss below, the pentagram map is defined on the so-called twisted polygons. The pentagram map commutes with projective transformations and thereby induces a map on spaces of projective equivalence classes of polygons, both ordinary and twisted.

In recent years, the pentagram map has attracted a lot of attention, thanks to the following developments.

1. In [Sch3], I found a hierarchy of integrals to the pentagram map, similar to the KdV hierarchy. I also related the pentagram map to the octahedral recurrence, and observed that the continuous limit of the pentagram map is the classical Boussinesq equation. For later reference, call the pentagram integrals the *monodromy invariants*.
2. In [OST1], Ovsienko, Tabachnikov and I showed that the pentagram map is a completely integrable system when defined on the space of projective classes of twisted polygons. We also elaborated on the connection to the Boussinesq equation. The main new idea is the introduction of a pentagram-invariant Poisson bracket with respect to which the monodromy invariants commute.
3. In [Sol] Soloviev showed that the pentagram map is completely integrable, in the algebro-geometric sense, on spaces of projective classes of real polygons and on spaces of projective classes of complex polygons. In particular Soloviev showed that the pentagram map has a Lax

pair and he deduced the invariant Poisson structure from the Phong-Krichever universal formula.

4. In [OST2] (independently, at roughly the same time as [Sol]) Ovsienko, Tabachnikov and I showed that the pentagram map is a discrete, completely integrable system, in the sense of Liouville-Arnold, when defined on the space of projective classes of closed convex polygons.
5. In [Gli1], Glick identified the pentagram map with a specific cluster algebra, and found algebraic formulas for iterates of the map which are similar in spirit to those found by Robbins and Rumsey for the octahedral recurrence. See also [Gli2].
6. In [GSTV], Gekhtman, Shapiro, Tabachnikov, Vainshtein generalized the pentagram map to similar maps using longer diagonals, and defined on spaces of so-called *corrugated polygons* in higher dimensions. The work in [GSTV] generalizes Glick's cluster algebra.
7. In [MB1], Mari-Beffa defines higher dimensional generalizations of the pentagram map and relates their continuous limits to various families of integrable PDEs. See also [MB2].
8. In recent work, [KS1], [KS2], and [KS3], Khesin and Soloviev obtain definitive results about higher dimensional analogues of the pentagram map, their integrability, and their connection to KdV-type equations.
9. In the preprint [FM], Fock and Marshakov relate the pentagram map to, among other things, Poisson Lie groups.
10. The preprint [DiFK] discusses many aspects of the octahedral recurrence, drawing connections to the work in [GSTV].

Though this is not directly related to the pentagram map, it seems also worth mentioning the recent paper [GK] of Goncharov and Kenyon, who study a family of cluster integrable systems. These systems are closely related to the octahedral recurrence which, in turn, is closely related to the pentagram map.

A *Poncelet polygon* is a polygon which is simultaneously inscribed in, and circumscribed about, a conic section. Two Poncelet polygons are *in*

the same family, or related, if they are simultaneously inscribed in the same conic and circumscribed about the same conic. The famous *Poncelet porism* says that any Poncelet polygon is related to a 1-parameter family of Poncelet polygons. What is remarkable here is that the related polygons typically are not projectively equivalent.

The pentagram map interacts nicely with Poncelet polygons. Recall that $T^2(P)$ is the image of P under the square of the pentagram map, considered as a labeled polygon in a canonical way. The following theorem is a consequence of the results in [Sch4], and also a consequence of a classical result of Darboux:

Theorem 1.1 *Let $P, Q \in \mathcal{C}$ be related Poncelet polygons. Then there is a projective transformation (the same for P and Q) which carries $T^2(P)$ to P and $T^2(Q)$ to Q and respects the labelings.*

Note that Theorem 1.1 make two statements. First, the image of a Poncelet polygon under the square of the pentagram map is projectively equivalent to the original polygon. Second, one and the same projective equivalence works for a pair of related Poncelet polygons.

Let \mathcal{C}_n denote the space of labeled projective equivalence classes of strictly convex real n -gons. A *Poncelet point* in \mathcal{C}_n is an equivalence class of Poncelet polygons. Theorem 1.1 shows that T^2 fixes every Poncelet point in \mathcal{C}_n . Every pentagon is a Poncelet polygon, and in fact there is a suitable labeling convention with respect to which T is the identity on \mathcal{C}_5 . This classical fact was known to Motzkin [M] and perhaps goes back even further. On \mathcal{C}_6 , the map T^2 is the identity with respect to a labeling convention that is different than the one discussed above: $T^2(P)$ and \tilde{P} are projectively equivalent, where \tilde{P} is obtained from P by cycling the vertex labels by 3. For $n \geq 7$, the action of T^2 on \mathcal{C}_n is not periodic.

The purpose of this paper is to study a deeper and more subtle connection between the pentagram map and Poncelet polygons.

Theorem 1.2 (Main) *Any two related Poncelet polygons have the same monodromy invariants.*

For convenience, we will prove Theorem 1.2 when n is even and large, say $n > 10$. The odd case has a proof similar to the even case. The case for small n , either even or odd, is similar to the case for large n , but the argument is somewhat less transparent.

Our proof is an argument in complex analysis. When defined over \mathbf{C} , the generic Poncelet family – i.e., a collection of mutually related Poncelet polygons – is naturally parametrized by a complex torus ¹ \mathbf{T} . The monodromy functions are meromorphic functions on \mathbf{T} , and our goal is to show that these functions are all constant. Our technique is to analyze the potential poles of the functions, which correspond to the singular Poncelet polygons within the family. We show that the functions are all bounded in neighborhoods of the singular Poncelet polygons, thereby showing that there are no poles at all. Consequently, all the functions must be constant.

Here is an overview of the paper. In §2 we discuss background and preliminary material. In §3, we reduce Theorem 1.2 to two technical lemmas, Lemma 3.8 and Lemma 3.9. The rest of the paper is devoted to proving these two lemmas. In §4 we provide some information, a mixture of classical and perhaps new, concerning Poncelet polygons and their degenerations. In §5 we prove Lemma 3.8. In §6 we prove Lemma 3.9.

I'd like to thank Valentin Ovsienko and Sergei Tabachnikov for many interesting discussions about the pentagram map. I would also like to thank the IHES and Caltech for their support during the writing of an early version of this paper.

¹By *complex torus*, we mean a compact Riemann surface which is holomorphically equivalent to \mathbf{C}/Λ , where Λ a planar lattice.

2 Preliminaries

2.1 Coordinates for Polygons

A *twisted n -gon* is a bi-infinite sequence $\{P_i\}$ of points in the (real) projective plane \mathbf{P} such that

$$P_{k+n} = M \circ P_k \quad \forall k. \quad (1)$$

for some projective transformation M . The map M is called the *monodromy* of P . The space \mathcal{P}_n is the space of twisted polygons modulo projective transformation. When M is the identity, we can interpret a twisted n -gon as an ordinary polygon. Hence \mathcal{C}_n is a subvariety of \mathcal{P}_n . Our paper [OST2] gives equations for this subvariety.

A *flag* of P is a pair (p, L) , where p is a vertex of P and L is one of the two lines of P incident to v . Figure 2.1 shows how we order the flags.

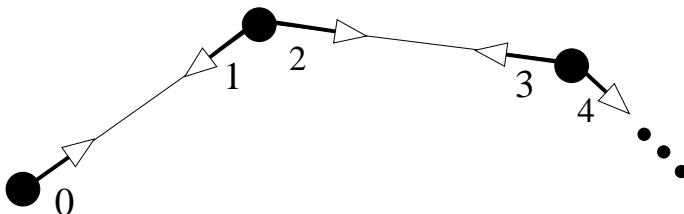


Figure 2.1: Flags of P .

We have the *inverse cross ratio*

$$\chi(a, b, c, d) = \frac{(a - b)(c - d)}{(a - c)(b - d)}. \quad (2)$$

To each flag $F = F_k$ we associate the cross ratio x_k of the 4 white points, as shown in Figure 2.2.

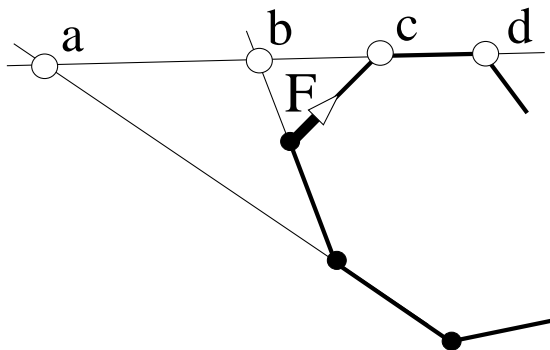


Figure 2.3: Geometry of the Corner Invariants

This construction associates a $2n$ periodic list $\dots, x_0, x_1, x_2, \dots$ to P . We usually just write x_1, \dots, x_{2n} , taking a single period. Sometimes x_1, \dots, x_{2n} determines a closed polygon, and sometimes not.

Vertex and Flag Conventions: Sometimes we find it convenient to use the variable names $x_1, y_1, x_2, y_2, \dots$ in place of the variables $x_1, x_2, x_3, x_4, \dots$. (So, $\text{new}(y_1) = \text{old}(x_2)$ and $\text{new}(x_2) = \text{old}(x_3)$, etc.) We call the list x_1, x_2, x_3, \dots the *flag coordinates* of the polygon and we call the list $x_1, y_1, x_2, y_2, \dots$ the *vertex coordinates* of the polygon. These vertex coordinates are used in [OST1] and [ST] while the flag coordinates are used in [S3] and [OST2]. In the vertex coordinates, the variables x_k and y_k are associated to the vertex P_k . In the flag coordinates, the variable x_k is associated to the k th flag.

2.2 Flag Coordinates for Poncelet Polygons

A poncelet polygon is *nondegenerate* if its points are pairwise distinct.

Lemma 2.1 *The flag coordinates of a non-degenerate Poncelet polygon all lie in the set $\mathbf{C} - \{0, 1\}$.*

Proof: Let P be a non-degenerate Poncelet polygon. Our proof refers to Figure 2.2. If the flag coordinate in Figure 2.2 equals one of $(0, 1, \infty)$, then the points a, b, c, d are not all distinct. In this case, either two vertices of P coincide, or 3 vertices are collinear. The former case is a direct contradiction, and the latter case contradicts the fact that a line intersects a conic in at most 2 points. ♠

Though we do not need it in this paper, we mention a consequence of [S3, Lemma 4.1].

Theorem 2.2 *Let P be an n -gon with flag coordinates x_1, \dots, x_{2n} . Then P is a Poncelet polygon if and only if there is a single value $H(P)$ such that*

$$H(P) = (1 - x_{i-1})x_i(1 - x_{i+1}), \quad \forall i. \quad (3)$$

Moreover, if P and Q are related Poncelet polygons, then $H(P) = H(Q)$.

It seems that Theorem 2.2 would be useful in proving the main result of this paper. However, we haven't found a way to use it. Also, it seems that one could express the monodromy invariants for Poncelet polygons directly in terms of H . We have not done this.

2.3 The Pentagon Map

As we mentioned above, the pentagram map naturally acts on twisted polygon as well as on closed polygons. One basic fact is that the pentagram map is monodromy preserving. That is, if P is a twisted polygon with monodromy M , then so is the image of P under the pentagram map. This follows immediately from the projective naturality of the pentagram map.

The second important property is algebraic. Let T^2 be the square of the pentagram map. In [S3] we show that (in flag coordinates.)

$$T^2 = \alpha_1 \circ \alpha_2. \quad (4)$$

Here $\alpha_1(x_1, \dots, x_{2n}) = (x'_1, \dots, x'_{2n})$ and $\alpha_2(x_1, \dots, x_{2n}) = (x''_1, \dots, x''_{2n})$ where

$$\begin{aligned} x'_{2k-1} &= x_{2k} \frac{1 - x_{2k+1}x_{2k+2}}{1 - x_{2k-3}x_{2k-2}}; & x'_{2k} &= x_{2k-1} \frac{1 - x_{2k-3}x_{2k-2}}{1 - x_{2k+1}x_{2k+2}}; \\ x''_{2k+1} &= x_{2k} \frac{1 - x_{2k-2}x_{2k-1}}{1 - x_{2k+2}x_{2k+3}} & x''_{2k} &= x_{2k+1} \frac{1 - x_{2k+2}x_{2k+3}}{1 - x_{2k-2}x_{2k-1}} \end{aligned} \quad (5)$$

From the formulas above, we see that the pentagram map commutes with a certain “rescaling” operation. Define

$$R_t(x_1, x_2, x_3, x_4, \dots) = (tx_1, t^{-1}x_2, tx_3, t^{-1}x_4, \dots). \quad (6)$$

We have

$$R_t \circ T^2 = T^2 \circ R_t. \quad (7)$$

2.4 The Monodromy Invariants

We state our formulas using the flag coordinates. Here we give formulas for the integrals which arise in our main theorem. These formulas are not needed for our proof, but we discuss them for completeness. (The disinterested reader can safely skip this section.) This material also appears in [S3], with slightly different notation.

We say that a *odd block* is a sequence either of the form a or of the form $a, a+1, a+2$, where a is odd. We say that two odd blocks are *well separated* if there are at least 3 integers separating them, reckoned cyclically. (Thus, 1 and $2n-1$ are adjacent odd integers.) For instance 1 and 3, 4, 5 are not well separated, but 1 and 5, 6, 7 are well separated (when n is large.)

We say that an *odd admissible subset* is a finite subset of $\{1, \dots, 2n\}$ that decomposes into pairwise well-separated odd blocks. We define the *sign* of an odd admissible sequence to be $(+)$ if there are an even number of singles and $(-)$ if there are an odd number of singles. For instance $(1, 5, 6, 7, 11)$ has sign $(+)$. The emptyset counts as an admissible sequence, and its sign is $(+)$. We define the *weight* to be the number of odd blocks in the sequence. For instance, $(1, 5, 6, 7, 11)$ has weight 3.

We attach a monomial to each odd admissible sequence I , as follows.

$$m(I) = \text{sign}(I)x^I. \quad (8)$$

As we mentioned above, we take n even for convenience. Given any $k = 1, \dots, n/2$ we define S_k to be the set of odd admissible sequences of weight k . We then define

$$O_k = \sum_{I \in S_k} m(I). \quad (9)$$

We define the invariant E_k similarly, except that we use even blocks and even admissible sequences; these are defined by interchanging the roles of odd and even in the construction above. Finally, for completeness, we define

$$O_n = x_1 x_3 x_5 \dots x_{2n-1}; \quad E_n = x_2 x_4 x_6 \dots x_{2n}. \quad (10)$$

Though we do not need it for this paper, we mention a recent result in [ST].

Theorem 2.3 *Suppose that P is inscribed in a conic section or circumscribed about a conic section. Then $O_k(P) = E_k(P)$ for all k .*

This result holds, in particular, when P is a Poncelet polygon.

2.5 Relations Amongst the Monodromy Invariants

For the purposes of proving Theorem 1.2, we don't need the above explicit formulas for the monodromy invariants. Now we formulate things in a way that is more useful for our present purposes.

Let M be the monodromy of our twisted polygon P , as in Equation 1. We lift M to an element of $GL_3(\mathbf{R})$ which we also denote by M . We define

$$\Omega_1 = \frac{\text{trace}^3(M)}{\det(M)}; \quad \Omega_2 = \frac{\text{trace}^3(M^{-1})}{\det(M^{-1})}. \quad (11)$$

These quantities are independent of the lift of M and only depend on the conjugacy class of M . Finally, these quantities are invariant under the pentagram map, because the pentagram map is monodromy-preserving.

We define

$$\tilde{\Omega}_1 = O_n^2 E_n \Omega_1; \quad \tilde{\Omega}_2 = O_n E_n^2 \Omega_2. \quad (12)$$

We say that a polynomial in the flag coordinates has *weight* k if

$$R_t^*(P) = t^k P. \quad (13)$$

Here R_t^* denotes the obvious action of R_t on polynomials. The significance of the quantities O_k and E_k is that they have weight k and $-k$ respectively. That is, they are *homogeneous* with respect to this weighting system.

In [S3] we show that

$$\tilde{\Omega}_1 = \left(\sum_{k=0}^{n/2} O_k \right)^3; \quad \tilde{\Omega}_2 = \left(\sum_{k=0}^{n/2} E_k \right)^3. \quad (14)$$

Now we explain briefly why O_k and E_k really are invariants of T^2 . The map T^2 is monodromy preserving, so T^2 preserves both Ω_1 and Ω_2 . Also, from the formula for T^2 , we see that T^2 preserves both E_n and O_n . Hence T^2 preserves both $\tilde{\Omega}_1$ and $\tilde{\Omega}_2$. Since T^2 commutes with the scaling operation R_t , we see that T^2 preserves the weighted homogeneous pieces of $\tilde{\Omega}_1$ and $\tilde{\Omega}_2$. Hence E_k and O_k really are invariants of T^2 , for all k .

3 Outline of the Proof

3.1 Reduction to Two Lemmas

First we state Theorem 1.2 more precisely.

Theorem 3.1 *Let P and Q be and two related Poncelet polygons. Then we have $E_k(P) = E_k(Q)$ and $O_k(P) = O_k(Q)$ for all k .*

We will deduce Theorem 3.1 from two lemmas. Let R_t denote the scaling operation defined in §2.3. Let $P_t = R_t(P)$ and likewise define $Q_t = R_t(Q)$. Note that P_t and Q_t are to be interpreted as twisted polygons. If P has flag coordinates (x_1, x_2, \dots) then P_t has flag coordinates $(tx_1, t^{-1}x_2, tx_3, t^{-1}x_4, \dots)$. Technically, just the projective equivalence class of P_t and Q_t is well-defined. However, when it comes up, we will concretely specify some way to get actual twisted polygons.

Here are the two technical lemmas.

Lemma 3.2 $E_n(P) = E_n(Q)$ and $O_n(P) = O_n(Q)$.

Lemma 3.3 $\Omega_1(P_t) = \Omega_1(Q_t)$ and $\Omega_2(P_t) = \Omega_2(Q_t)$ for all t sufficiently close to 1.

Proof of Theorem 3.1: We have the general homogeneity relations:

$$E_k(P_t) = t^k E_k(P); \quad O_k(P_t) = t^{-k} O_k(P). \quad (15)$$

Lemma 3.2 combines with Equation 15 to give

$$E_n(P_t) = E_n(Q_t); \quad O_n(P_t) = O_n(Q_t), \quad \forall t. \quad (16)$$

We introduce the symbol $\bowtie t$ to mean “for all t sufficiently close to 1.” Lemma 3.3 says, in particular,

$$\Omega_1(P_t) = \Omega_1(Q_t) \quad \bowtie t. \quad (17)$$

Combining this with Equations 12 and 16, we get

$$\tilde{\Omega}_1(P_t) = \tilde{\Omega}_1(Q_t) \quad \bowtie t. \quad (18)$$

Combining this with Equation 14, we see that

$$\sum_{k=1}^{n/2} t^k (E_k(P) - E_k(Q)) = 0 \quad \asymp t. \quad (19)$$

But then we have a polynomial with infinitely many roots. Hence, all the coefficients are 0. That is, $E_k(P) = E_k(Q)$ for all k . Similarly $O_k(P) = O_k(Q)$ for all k . ♠

3.2 Some Basic Complex Analysis

We are going to use some complex analysis to prove Lemmas 3.2 and 3.3. Here we recall some basic facts from complex analysis.

By a *complex torus*, we mean a compact Riemann surface biholomorphically equivalent to \mathbf{C}/Λ , where Λ is a planar lattice. As is well known, a globally defined holomorphic function on a compact Riemann surface must be constant. We will use the principle several times in our proof.

A complex torus \mathbf{T} has a natural unit area flat metric, coming from the description as \mathbf{C}/Λ . Any point $z_0 \in \mathbf{T}$ has a coordinate chart $\text{int } \mathbf{C}$, a local isometry, which carries z_0 to 0. We call these coordinate charts *isometric coordinates*. They are canonical up to rotations.

Suppose that $f : \mathbf{T} \rightarrow \mathbf{C}$ is *meromorphic*, i.e. defined and holomorphic except at finitely many points of \mathbf{T} , called *poles*. We say that $z_0 \in \mathbf{T}$ is a *Laurent pole* if, in isometric coordinates about z_0 , the function f has the form

$$f(z) = \sum_{k=-N}^{-1} C_k z^k + h(z), \quad (20)$$

where $h(z)$ is holomorphic in a disk about the origin.

Lemma 3.4 *Let d denote the flat metric on \mathbf{T} . Suppose f is meromorphic on \mathbf{T} and z_0 is a pole of f . Suppose also that $|f(z)| \leq Cd(z, z_0)^{-m}$ for some constant C and some integer m . Then z_0 is a Laurent pole of f .*

Proof: In isometric coordinates, we have the bound $|f(z)| \leq C|z|^{-m}$. As is well known, this implies that f has a finite Laurent series in a neighborhood of 0. ♠

Lemma 3.5 *Suppose that f is a meromorphic function on \mathbf{T} and f has a Laurent pole at z_0 . Suppose that there is an infinite sequence of points $\{z_n\} \in \mathbf{T}$ such that $z_n \rightarrow z_0$ and $|f(z_n)|$ is bounded. Then f can be defined (uniquely) at z_0 so that the extension is holomorphic in a neighborhood of z_0 .*

Proof: In isometric coordinates, f has a Laurent series expansion as in Equation 20. The conditions of the lemma imply that there is a sequence $\{z_n\}$ converging to 0 so that $|f(z_n)|$ is bounded. This implies almost immediately that $C_{-N} = \dots = C_{-1} = 0$. ♠

3.3 The First Lemma

Now we reduce Lemma 3.2 to something more concrete. We start with a Poncelet polygon P which is inscribed in a conic C_1 and circumscribed about a conic C_2 . Over \mathbf{C} , the set of Poncelet polygons related to P is parametrized by a complex torus \mathbf{T} . See §4.2 for more details. One identifies the points on \mathbf{T} with *flags* (p, L) , where $p \in C_1$ and L is a line through p and tangent to C_2 . There are two kinds of Poncelet polygons in this family, *ordinary* and *degenerate*. The ordinary Poncelet polygons are those consisting of n distinct points in general position. The rest of the polygons we call *degenerate*. We classify the points of \mathbf{T} as *ordinary* and *degenerate*, according to the type of polygon they correspond to. There are finitely many degenerate points.

Let P_z be the Poncelet polygon corresponding to the point $z \in \mathbf{T}$. Let $f : \mathbf{T} \rightarrow \mathbf{C}$ denote the function

$$f(z) = E_n(P^z). \tag{21}$$

Here P^z is the Poncelet polygon whose 1st and 2nd vertices determine the flag associated to z . The vertex of the flag is $V^z(1)$ and the line contains $V^z(1)$ and $V^z(2)$.

Lemma 3.6 *f is holomorphic in a neighborhood of each ordinary point.*

Proof: At an ordinary point, z , the corresponding Poncelet polygon P^z is non-degenerate. The corner invariants are well defined and finite, by Lemma 2.1, and depend holomorphically on z . ♠

Lemma 3.7 *Every degenerate point of \mathbf{T} is a Laurent pole for f .*

Proof: Let z_0 be a degenerate point of \mathbf{T} . Let d be the flat metric on \mathbf{T} . We have a double holomorphic branched cover $\pi : \mathbf{T} \rightarrow C_1$. Locally such a map is either bi-Lipschitz or looks like $z \rightarrow z^2$. Therefore, there is some constant K_1 so that

$$\|\pi(z) - \pi(z_0)\| \geq K_1 d(z, z_0)^2. \quad (22)$$

At the same time, the points, lines, and cross ratios involved in the definition of the flag coordinates of P_z are obtained by taking, finitely many times, rational functions and square roots of the coordinates of $E(z)$. Hence, we have a bound

$$|f(z)| \leq K_2 |\pi(z) - \pi(z_0)|^{-m} \quad (23)$$

for some constant K_2 and some positive integer m . Combining our two bounds, we get

$$|f(z)| \leq K_3 d(z, z_0)^{-2m}. \quad (24)$$

Our result now follows from Lemma 3.4. ♠

We will prove the following result in §4.

Lemma 3.8 *For each degenerate point $z \in \mathbf{T}$ there is a sequence $\{z_j\}$ of ordinary points such that $z_j \rightarrow z$ and $\{f(z_j)\}$ is bounded.*

Combining Lemmas 3.5, 3.7, and 3.8, we see that f extends to be holomorphic in a neighborhood of each degenerate point. But then this extension is holomorphic on \mathbf{T} . As we mentioned above, a holomorphic function on a compact Riemann surface is constant. Hence f is constant. This proves Lemma 3.2.

Remark: When it comes time to prove Lemma 3.8, we will consider the case when C_1 is the unit circle and C_2 is a concentric (but not circular) ellipse contained in the unit disk. By analytic continuation, it suffices to consider this case. We make this restriction because it will help us get a nice picture of what is going on. The same goes for our proof of Lemma 3.9 below.

3.4 The Second Lemma

We will take a similar approach to Lemma 3.3. For $w \in \mathbf{T}$ a regular point, we let P_t^w be the t -rescaled version of the polygon P^w . Note that P_t^w is not a polygon, but rather a twisted polygon. Define the functions

$$g_t(z) = \Omega_1(P_t^z), \quad h_t(z) = \Omega_2(p_t^z). \quad (25)$$

Suppose that $z \in \mathbf{T}$ is a degenerate point. We call z *special* if z has the following property. If t is sufficiently close to 1 then there is a sequence $\{z_j\}$, converging to z , such that

- $P_t^{z_j}$ exists and has monodromy matrix $M_t^{z_j}$.
- The limit $M = \lim_{j \rightarrow \infty} M_t^{z_j}$ exists and lies in $GL_3(\mathbf{R})$.

If z is special, then same argument as in the proof of Theorem 3.2 says that the functions g_t and h_t are holomorphic in a neighborhood of z , for all t sufficiently close to 1.

There is an action of D_n , the order $2n$ dihedral group, on \mathbf{T} , such that the orbits are exactly the flags corresponding to Poncelet polygons. We describe this action in §4.2. We call two points of \mathbf{T} *equivalent* if they are in the same D_n -orbit. In §5 we prove the following result.

Lemma 3.9 *For each degenerate point z' there is an equivalent degenerate point z which is special.*

Let t be sufficiently close to 1. Lemma 3.9 combines with the basic complex analysis, as in the previous section, to show that g_t and h_t are holomorphic in a neighborhood of a special point. Lemma 3.9 covers one degenerate point per equivalence class, and the unordered pair $\{g_t, h_t\}$ is constant on D_n -orbits. Hence, g_t and h_t are holomorphic in neighborhoods of all the singular points. Hence, they are constant. This proves Lemma 3.3.

Remark: The difficulty in Lemma 3.9 is that, even for t near 1, some of the coordinates for the Poncelet polygon blow up. This makes the twisting operation potentially very violent, even for t near 1. What we will show is that, in fact, the twisting operation is very gentle even though some of the invariants are blowing up.

The rest of the paper is devoted to proving Lemmas 3.8 and 3.9.

4 Poncelet Polygons and their Degenerations

4.1 Conics

We recall the set-up from §3.1. For the purposes of proving Theorem 3.1 it suffices to consider the case when P is inscribed in a conic C_1 and circumscribed about a conic C_2 , with the following equations.

$$C_1 : \quad x^2 + y^2 = 1. \quad (26)$$

$$C_2 : \quad ax^2 + by^2 = 1., \quad 1 < a < b. \quad (27)$$

The intersection $C_1 \cap C_2$ (over \mathbf{C}) consists of 4 points. Let $X \subset \mathbf{CP}^2$ be the copy of \mathbf{RP}^2 containing the real affine plane $\{(x, iy) | x, y \in \mathbf{R}\}$. If we identify X with \mathbf{RP}^2 using the map $(x, iy) \rightarrow (x, y)$, then $C_1 \cap X$ is the hyperbola $x^2 - y^2 = 1$ and $C_2 \cap X$ is the hyperbola $ax^2 - by^2 = 1$. These two hyperbolas intersect in 4 points.

Drawing a pair of hyperbolas is not so useful for our purposes. We can identify X with the real projective plane, and then apply a suitable real projective transformation so that $C_1 \cap X$ and $C_2 \cap X$ are intersecting ellipses, as shown in Figure 4.1.

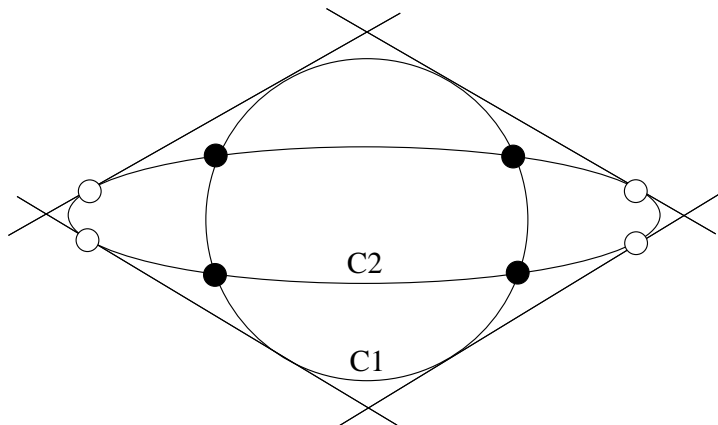


Figure 4.1: all the branch points

In Figure 4.1 we have distinguished 8 points. The 4 black points are the points of $C_1 \cap C_2$. The 4 white points are the tangent points on C_2 , contained in the 4 lines that are mutually tangent to C_1 and C_2 . These 8 points play a special role in our analysis.

4.2 The Complexified Picture

Let \mathbf{T} be the complex torus consisting of flags (p, L) , where $p \in C_1$ and L is tangent to C_2 . For $j = 1, 2$ we have maps $\phi_j : \mathbf{T} \rightarrow C_j$ given by

$$\phi_1(z) = p; \quad \phi_2(z) = L \cap C_2; \quad z = (p, L). \quad (28)$$

Both ϕ_1 and ϕ_2 are double branched-covers. The map ϕ_1 is branched over the 4 points of $C_1 \cap C_2$. These are the black points in Figure 4.1. The map ϕ_2 is branched over each of the 4 points of $x \in C_2$ such that the line tangent to C_2 at x is also tangent to C_1 . These are the white points in Figure 4.1.

The *singular points* of ϕ_j are the pre-images of the branch points. There are 4 such points. In its flat metric, \mathbf{T} is obtained by gluing the opposite sides of a rectangle in the obvious way. Referring to Figure 4.2, the black points indicate the singular points of ϕ_1 and the white points indicate the singular points of ϕ_2 . Reflection in the vertical centerline swaps black and white points. The dotted horizontal lines are $\phi_1^{-1}(C_1 \cap \mathbf{R}^2)$.

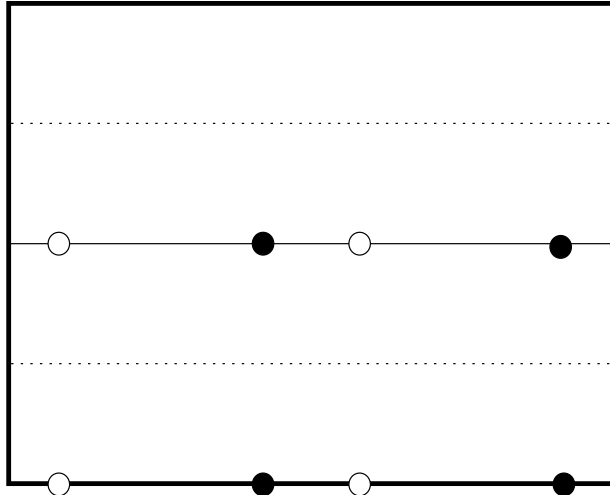


Figure 4.2: singular points

There are two natural involutions associated with this picture. The map I_1 has the action

$$I_1(p, L_1) = (p, L_2). \quad (29)$$

Here L_1 and L_2 are the two lines such that (p, L_1) and (p, L_2) are flags. Geometrically, I_1 is an order 2 rotation about the black singular points in \mathbf{T} .

Similarly, the map I_2 has the action

$$I_2(p_1, L) = (p_2, L). \quad (30)$$

Geometrically, I_2 is an order 2 rotation about the white singular points in \mathcal{T} . Evidently, the map I_j commutes with the map ϕ_j . That is

$$\phi_j \circ I_j = \phi_j; \quad j = 1, 2. \quad (31)$$

The group $D_n = \langle I_1, I_2 \rangle$ is the dihedral group of order $2n$. The map ϕ_1 maps the D_n -orbits to Poncelet polygons. The Poncelet polygon is ordinary iff its image has n points. This happens iff the orbit does not contain one of the singular points of ϕ_1 or ϕ_2 . Thus, there are $4n$ degenerate points. Each degenerate point is equivalent under D_n to one of the singular points. $2n$ of these degenerate points lie on the center horizontal line in Figure 4.2, hereafter called *the centerline* and denoted by Ξ . The other $2n$ lie on the bottom/top horizontal edge of the rectangle. By symmetry, it suffices to consider the ones on the centerline.

Figure 4.3 shows the degenerate points arranged along Ξ in case $n = 4$. The endpoints of Ξ are identified, so that Ξ is really a circle. The degenerate points on the Ξ are arranged into two D_n -orbits. One of the orbits consists of the black points and the other orbit consists of the white points. This picture is representative of the cases when n is even.

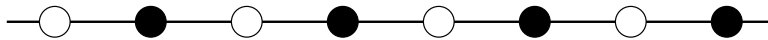


Figure 4.3: degenerate points on the centerline

4.3 The Singular Orbits

The map $\phi_1 : \Xi \rightarrow C_1 \cap X$ is a 2-to-1 folding map. If we suitably normalize the picture in Figure 4.1, the 2 singular points on Ξ are mapped to the two upper black points of $C_1 \cap C_2 \cap X$, and $\phi_1(\Xi)$ is the circular arc in Figure 4.1 connecting these upper black points. Outside any neighborhood U of the two singularities of ϕ_1 , the map ϕ_1 is C_U -bilipschitz. Here C_U depends on the neighborhood U . Here Ξ is given its flat metric and $C_1 \cap X$ is given a metric which makes it into a round circle, as in Figure 4.1.

We denote the singular orbits on Ξ by Ψ_1 and Ψ_2 . These orbits have the following description.

1. Ψ_1 is the D_n -orbit of the 2-singularities of ϕ_1 that lie on Ξ – the black points in Figure 4.2. The restriction of ϕ_1 to Ψ_1 is 2-to-1 on all but 2 points of this orbit. The image $\phi_1(\Psi_1)$ consists of $(n/2) + 1$ points.
2. Ψ_2 is the D_n -orbit of the 2-singularities of ϕ_2 that lie on Ξ – the white points in Figure 4.2. In this case, $\phi_1(\Psi_2)$ maps this orbit to C_1 in a 2-to-1 fashion.

Given the folding nature of ϕ_1 , Figure 4.4 shows a fairly accurate picture of one end of $\phi_1(\Psi_1)$ and $\phi_1(\Psi_2)$. The other end is the mirror reflection. The points in the middle are not really of interest to us. In the first case, the point labelled 5 is the branch point.

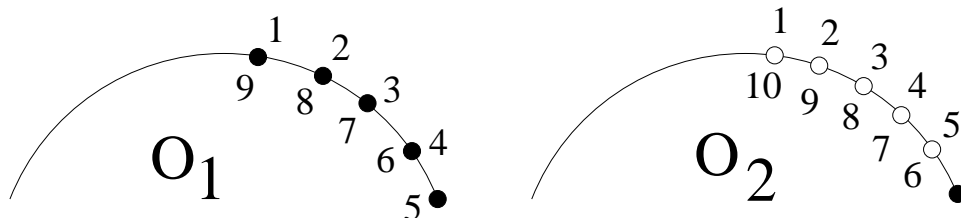


Figure 4.4: local picture of the degenerate polygons

4.4 A Bi-Lipschitz Model for Perturbations

For small ϵ , we let Ψ_j^ϵ be the D_n -orbit that is ϵ away from Ψ_j . the perturbed orbit Ψ_j^ϵ is obtained by replacing each point of Ψ_j by two points, on either side, that are 2ϵ apart. Our goal is to explain the geometry of the Poncelet polygons $\phi_1(\Psi_j^\epsilon)$, in a sufficiently accurate approximate sense.

The picture of $\phi_1(\Psi_2^\epsilon)$ is easier to understand. Each of the points labelled $(5, 6)$, $(4, 7), \dots$ is split apart into two points. These points are spaced between $C^{-1}\epsilon$ and $C\epsilon$ apart, and the distance between the point pairs is at least C^{-1} . Here C is a positive constant that only depends on n .

The picture of the image $\phi_1(\Psi_1^\epsilon)$ is obtained by replacing the points commonly labelled $(1, 9)$ $(2, 8)$, $(3, 7)$ and $(4, 6)$ each by two points that are between $C^{-1}\epsilon$ and $C\epsilon$ apart and by moving the point labelled 5 by a distance of at most $C\epsilon^2$.

All the distance estimates, except the last one, come from the fact that ϕ_1 is bi-lipschitz away from any neighborhood of a singular point. The estimate on the motion on the point labelled 5 comes from the fact that $\phi_1(z) = z^2$

in a neighborhood of a singular point, when written in suitable holomorphic coordinates.

We find it convenient to apply a projective transformation that moves C_1 to the standard parabola

$$\Pi = \{(x, y) \mid y = x^2\} \tag{32}$$

and carries the rightmost points in our pictures to $(0, 0)$. Such a projective transformation is bi-lipschitz. To draw pictures in Π , we consider the projection onto the first coordinate. Figure 4.5 shows a fairly accurate picture of one end of (the renormalized image of) $\phi_1(\Psi_j^\epsilon)$. The top shows the case $j = 1$ and the bottom shows the case $j = 2$.

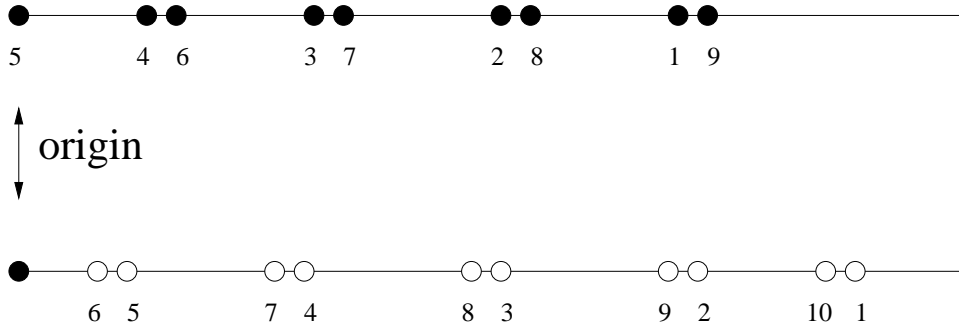


Figure 4.5: local model of the degenerations

The left endpoint is the origin. The only point we have not justified is the ordering of the points in Figure 4.5. The order we have drawn follows from the way D_n acts on Ξ . Alternatively, this order can be determined experimentally in one case; then the order remains unchanged in all cases by continuity. Again, we are showing the first coordinates of our points. They really lie on the parabola Π . Whether we consider the points on Π or just the first coordinates, the spacing between nearby points is between $C^{-1}\epsilon$ and $C\epsilon$, and the spacing between all other pairs of points is at least C^{-1} . Here C only depends on n .

Figure 4.5 gives us our local model for the way the Poncelet polygons degenerate at one end. The other end, halfway around in terms of the ordering on the points, is similar. The points in the middle play little role in the analysis, though sometimes we will have to consider these points in a very general sort of way.

5 Proof of Lemma 3.8

5.1 Reduction to Three Estimates

For the remainder of the paper, we use the vertex coordinates. That is, we use the variables $x_1, y_1, x_2, y_2, \dots$. Here x_k and y_k are the two vertex coordinates associated to the vertex P_k . We will just deal with the invariant $O_n = x_1 \dots x_n$. The case of E_n is entirely similar and indeed follows from symmetry. We have the formula

$$x_3 = \chi(V_1, V_2, (12)(34), (12)(45)). \quad (33)$$

Here $(12)(34)$ denotes the intersection of the line $\overline{P_1 P_2}$ with the line $\overline{P_3 P_4}$. The formulas for the other coordinates are obtained by shifting the indices.

For ease of exposition we will just consider the orbits Ψ_1^ϵ . The orbits Ψ_2^ϵ have an almost identical treatment, and indeed this second case follows from the first case and projective duality. We are interested in the invariants of the nearly singular Poncelet polygon

$$P^\epsilon = \phi_1(\Psi_1^\epsilon). \quad (34)$$

Here is a copy of the top line of Figure 4.5, which shows a model for this polygon. (Again, we have normalized so that P^ϵ is contained in the parabola $y = x^2$.)

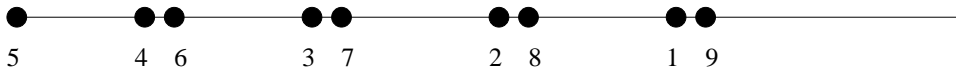


Figure 5.1: First coordinate projection of P^ϵ .

We will show that the product $x_3 x_4 x_5$ remains bounded as $\epsilon \rightarrow 0$. For other nearby indices, the vertex coordinates involve 5 points that remain in general position even in the limit. The singularity at the other end has the same analysis. We need P to have at least 10 points so that the singularities at the two ends to not interfere at all with each other.

We use the usual notation $f \sim g$ to indicate that f/g lies between two positive constants that depend only on n . We will show that $x_4 \sim \epsilon$ and $x_5 \sim 1$ and $x_6 \sim 1/\epsilon$. Combining these estimates, we see that $x_4 x_5 x_6 \sim 1$. Hence, the product of interest to us remains bounded as $\epsilon \rightarrow 0$.

Our analysis in each case follows the same pattern. We will write

$$x_k = [a, b, c, d] \quad (35)$$

where a, b, c, d depend on both the index k and on ϵ . We will then analyze the geometry of a, b, c, d as $\epsilon \rightarrow 0$.

5.2 The First Estimate

The points of interest to us are shown in Figure 5.2. The points of interest to us are

$$a = V(2); \quad b = V(3); \quad c = L(23) \cap L(45); \quad d = L(23) \cap L(56).$$

Here $L(23)$ denotes the line through $V(2)$ and $V(3)$, etc. Looking at the picture, and using our model, we see that

$$\|c - d\| \sim \epsilon; \quad \|x - y\| \sim 1; \quad x \in \{a, b\} \quad y \in \{c, d\}. \quad (36)$$

Hence $x_4 \sim \epsilon$.

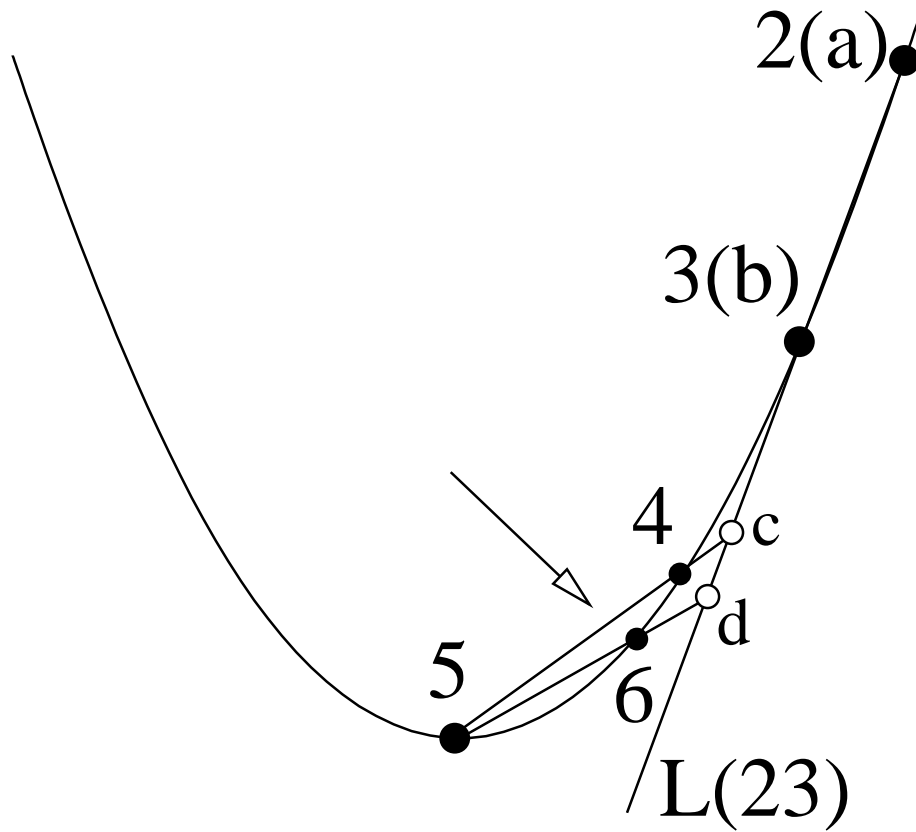


Figure 5.2: Estimating x_4 .

5.3 The Second Estimate

Figure 5.3 shows the situation for x_3 . The points of interest to us are

$$a = V(3); \quad b = V(4); \quad c = L(56) \cap L(34); \quad d = L(67) \cap L(34).$$

There is an (~ 1)-bilipschitz projective transformation that carries the points $V(3), V(7), V(4), V(6)$ to the vertices of a rectangle. (We mean that the transformation is (~ 1)-bilipschitz on the convex hull of these points.) From this, we conclude that

$$\|d - b\| \sim 1; \quad \|d - a\| \sim 1.$$

But then $\|d - c\| \sim 1$ as well. Also, $\|a - b\| \sim 1$ and $\|a - c\| \sim 1$. Hence $x_5 \sim 1$.

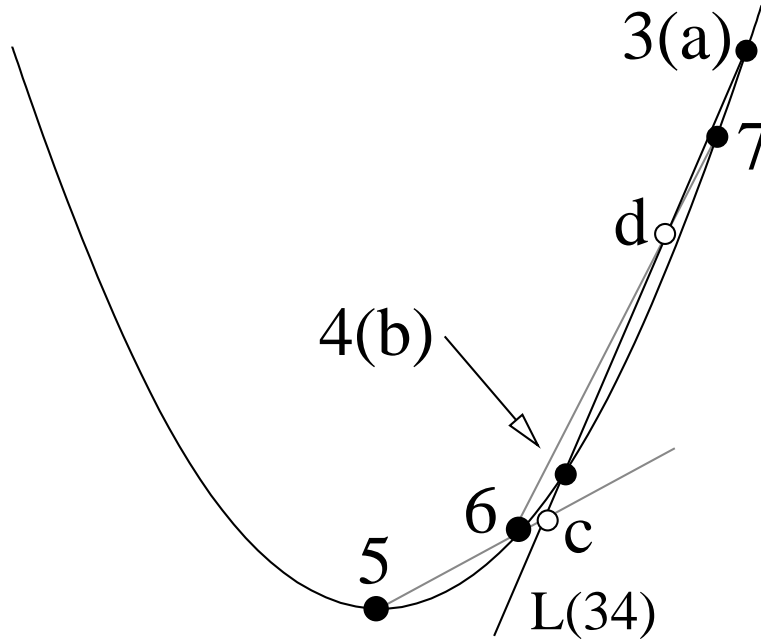


Figure 5.3: Estimating x_5 .

More is true in this case, since $\|b - c\| \sim \epsilon$ we conclude that

$$\left| 1 - \frac{\|a - b\|}{\|a - c\|} \right| \sim \epsilon; \quad \left| 1 - \frac{\|d - b\|}{\|d - c\|} \right| \sim \epsilon.$$

From this, we see that

$$\left| 1 - x_5(P^\epsilon) \right| \sim \epsilon. \tag{37}$$

5.4 The Third Estimate

Figure 5.4 shows the situation for x_6 . The points of interest to us are

$$a = V(4); \quad b = V(5); \quad c = L(67) \cap L(45); \quad d = L(78) \cap L(45).$$

In the same sense as the previous case, there is a uniformly bilipschitz projective map that carries $V(5), V(6), V(4), V(7)$ to a trapezoid whose 3 long sides have length 1 and whose short side has length ϵ . From this, we get

$$\|c - a\| \sim \epsilon. \quad (38)$$

Consider the triangle $(V(4), V(7), d)$. The small angles of this triangle are all ~ 1 . Also, one side of this triangle, namely the one connecting $V(4)$ to $V(7)$, has length ~ 1 . Hence all sides have length ~ 1 . In particular,

$$\|d - a\| \sim 1 \quad (39)$$

But then we have $\|c - d\| \sim 1$ and $\|b - d\| \sim 1$. Finally, $\|b - a\| \sim 1$. Hence $x_6 \sim \epsilon^{-1}$.

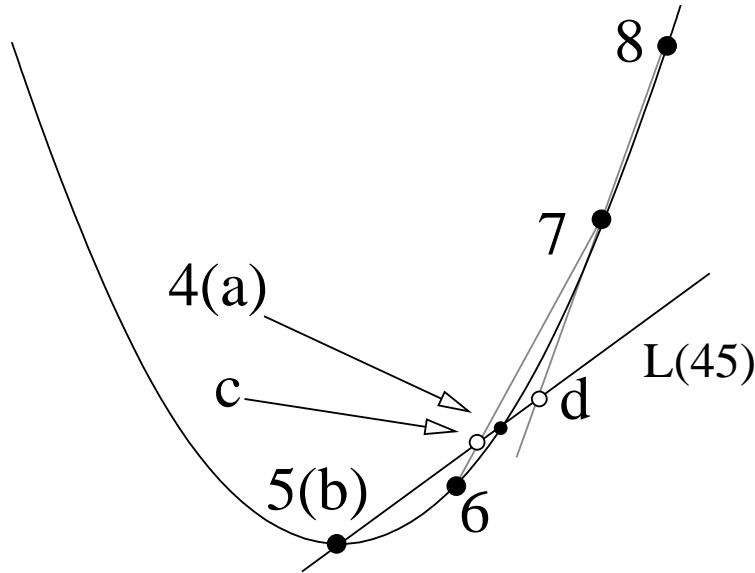


Figure 5.4: Estimating x_6 .

6 Proof of Lemma 3.9

6.1 A Continuity Principle

In this section we state a technical result which will help us prove Lemma 3.9. We use the vertex coordinates, as in the last chapter.

Lemma 6.1 *Let $\{P_k\}$ be a sequence of n -gons and let P be some fixed n -gon. Suppose that*

- $x_3(P_k) \rightarrow x_3(P) \in \mathbf{C} - \{0, 1\}$.
- $y_3(P_k) \rightarrow y_3(P) \in \mathbf{C} - \{0, 1\}$.
- $V_i(P_k) \rightarrow V_i(P)$ for $i = 1, 2, 3, 4$.

Then $V_5(P_k) \rightarrow V_5(P)$.

Proof: We know that $V_i(P_k) \rightarrow V_i(P)$ for $i = 1, 2, 3, 4$ and we want to show that $V_5(P_k) \rightarrow V_5(P)$. Adjusting the picture by a convergent sequence of projective transformations, we can normalize so that the first 5 vertices of P_k are

$$(0, 0), \quad (1, 0) \quad (1, 1); \quad (1, 0); \quad (a_k, b_k).$$

A direct calculation (leaving off the subscripts) shows that

$$a = \frac{(1 - x_3)y_3}{1 + (x_3 - 1)y_3}; \quad b = \frac{(1 - y_3)}{1 + (x_3 - 1)y_3}. \quad (40)$$

This shows how x_3 and y_3 determine the coordinates of V_5 . Our lemma is obvious from here. ♠

6.2 The Proof Modulo a Detail

We fix some even $n > 10$. As in the proof of Lemma 3.9, we need enough points to separate out the singularities at the two ends of our degenerate polygons. As in the proof of Lemma 3.8, we will just deal with the degenerations associated to the orbit Ψ_1 . The proof for the degenerations associated to Ψ_2 is essentially the same, and again follows from the first case and from projective duality.

We define

$$P^\epsilon = \phi_1(\Psi_1^\epsilon), \quad P_t^\epsilon = R_t(P^\epsilon). \quad (41)$$

The map R_t is the scaling transformation from Equation 6. As in §4.4, the polygon $\phi_1(\Psi_1^\epsilon)$ is the Poncelet polygon which is the image of the orbit Ψ_1^ϵ , the orbit which is ϵ away from the singular orbit Ψ_1 . Again, we reproduce the top line of Figure 4.5, which shows a model for P^ϵ .

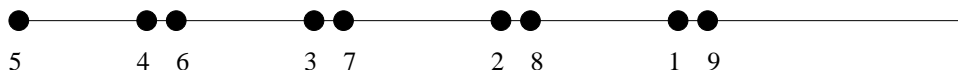


Figure 6.1: First coordinate projection of P_1^ϵ .

In constructing P_t^ϵ we normalize so that the vertices labelled 2, 3, 4, 5 are independent of t . Let $P = P^0$. Let $V_t^\epsilon(k)$ denote the k th vertex of P_t^ϵ .

Good Indices: We say that the index k is *good* if $V_{t_m}^{\epsilon_m}(k) \rightarrow V_1^0(k)$ for any sequence (ϵ_m, t_m) converging to $(0, 1)$.

By construction, the indices 2, 3, 4, 5 are good. In the next section we prove the following result.

Lemma 6.2 (Variation) *The indices 6, 7, 8 are good.*

We will assume this result, for now, and deduce some corollaries.

Lemma 6.3 *k is a good index for $k = 9, \dots, (n/2 + 5)$.*

Proof: We consider $k = 9$ first. Let x_1, y_1, \dots be the vertex coordinates. Given our model for P^ϵ , we have

$$x_7(P_m) \rightarrow x_7(P) \in (0, 1); \quad y_7(P_m) \rightarrow y_7(P) \in (0, 1).$$

We know that indices 5, 6, 7, 8 are good. The $k = 7$ case of Lemma 6.1 now shows that 9 is good. We can repeat the same argument, successively shifting the indices, to show that that k is a good index for 10, 11, $\dots, (n/2) + 5$. ♠

Remark: We can't go any further with a direct argument because the point $V_{n/2+5}(P)$, like $V_5(P)$, is a branch point. Put another way, the last vertex coordinates which don't degenerate are x_k and y_k for $k = n/2 + 3$. Put still another way, we encounter another "singularity" of P halfway through the index set, so we have to stop and take stock of what is going on.

Lemma 6.4 k is a good index for $k = 1, \dots, (n + 5)$.

Proof: The previous result establishes that $n/2 + k$ is a good index for $k = 2, 3, 4, 5$. Now we can re-normalize the picture, by a sequence of projective transformations converging to the identity, so that $V_{k+n/2}(P_m)$ is independent of n for $k = 2, 3, 4, 5$. Our analysis in the proof of Lemma 3.8 works equally well for the degeneracy corresponding to the index $(n/2) + 5$. So, the Variation Lemma implies that $k + n/2$ is a good index for $k = 6, 7, 8$. Now we can repeat the proof in the previous lemma so show that $n/2 + k$ is a good index for $k = 9, \dots, (n/2 + 5)$. ♠

Lemma 6.5 There exists a map $g : \mathbf{R} \rightarrow \mathbf{R} \cup \infty$ (not necessarily continuous) such that:

1. $\lim_{t \rightarrow 1} g(t) = 0$.
2. If $k \in \{2, \dots, n + 5\}$, then

$$\|V_t^\epsilon(k) - V_1^0(k)\| \leq g(t)$$

for all sufficiently small ϵ .

Proof: Suppose that this is false. Then there is some $\delta > 0$ with the following property: There is some sequence $\{t_m\}$ converging to 1 and some index $k \in \{2, \dots, n + 5\}$ such that $\|V_{t_m}^{\epsilon_m}(k) - V_1^0(k)\| > \delta$ for some $\epsilon_m < t_m$. But then the index k is not good. This is a contradiction. ♠

We say that a quadruple (A_1, A_2, A_3, A_4) of points in \mathbf{P} is δ -stable if the points (A'_1, A'_2, A'_3, A'_4) are in general position as long as $\|A'_j - A_j\| < \delta$ for $j = 1, 2, 3, 4$. Any general position quadrilateral in the plane is δ -stable for some $\delta > 0$.

Proof of Lemma 3.9: Looking at our models for the singular Poncelet polygons, we see that there is some $\delta > 0$ such that the two quads

$$\{V_1^0(a) | a = 2, 3, 4, 5\}, \quad \{V_1^0(a) | a = n + 2, n + 3, n + 4, n + 5\} \quad (42)$$

are 2δ -stable.

By Lemma 6.5, we can choose t sufficiently close to 1 so that

$$\|V_t^\epsilon(an + b) - V_1^0(an + b)\| \leq \delta, \quad a \in \{0, 1\}, \quad b \in \{2, 3, 4, 5\}. \quad (43)$$

Holding t fixed, we can choose a subsequence $\{\epsilon_j\}$ so that the the sequence of quads

$$\{V_t^{\epsilon_j}(a)|a = 2, 3, 4, 5\}, \quad \{V_t^{\epsilon_j}(a)|a = n + 2, n + 3, n + 4, n + 5\} \quad (44)$$

both converge to general position quads. The monodromy projective transformation $M_t^{\epsilon_j}$ converges to the projective transformation which carries the limit of the first quad to the limit of the second quad. Since both these limits are in general position, the limit map is a well-defined projective transformation. If we take representative matrices in $SL_3(\mathbf{R})$, we can get the convergence on the level of matrices. ♠

6.3 An Auxilliary Cross Ratio

The rest of the paper is devoted to proving the Variation Lemma.

Let $L(ij)$ denote the the line containing $V(i)$ and $V(j)$ and let $S(ij)$ be the slope of $L(ij)$. Let

$$z_5 = [S(35), S(45), S(65), S(75)]. \quad (45)$$

In general, we define z_1, z_2, \dots by shifting the indices. A calculation shows that

$$z_k = x_k y_k. \quad (46)$$

The importance of this quantity is that it does not change when we apply the map R_t , because $x_k \rightarrow tx_k$ and $y_k \rightarrow t^{-1}y_k$.

Now we consider the variation of one of these auxilliary cross ratios. As usual, we just consider the perturbation of Ψ_1 .

Lemma 6.6 $|1 - z_5(P^\epsilon)| < C\epsilon^2$ for some C that only depends on n .

Proof: From our model, $|S(35) - S(75)| \sim \epsilon$ and $|S(45) - S(65)| \sim \epsilon$, and all other pairs of slopes are ~ 1 apart. Our result now follows from the definition of the inverse cross ratio. ♠

6.4 The First Estimate

We treat the case $k = 6$ of the Variation Lemma. We use the coordinates z_1, z_2, \dots introduced in the previous section. First of all, we have

$$z_4(P_m) = z_4(P_{t_m}^{\epsilon_m}) = z_4(P^{\epsilon_m}). \quad (47)$$

The first equality is just a definition. The second equality comes from Equation 6 and Equation 46.

The indices 2, 3, 4, 5 correspond to points which do not move during our variation. Hence, $S(46)$ is the only m -dependent quantity in $z_4(P_m)$. Hence, it follows from Equation 47 that $L_m(46) \rightarrow L(46)$. Here $L(46)$ is the line tangent line to the parabola Π at $V(4) = V(6)$.

From Estimate 1 in the proof of Lemma 3.8, we have

$$\chi(a, b, c, d_m) = x_4(P_m) \sim \epsilon_m. \quad (48)$$

Hence $d_m \rightarrow c$. Since $L_m(46) \rightarrow L(46)$, the fact that $d_m \rightarrow c$ implies that $V_m(6) \rightarrow V(4) = V(6)$. This gives the Variation Lemma for $k = 6$.

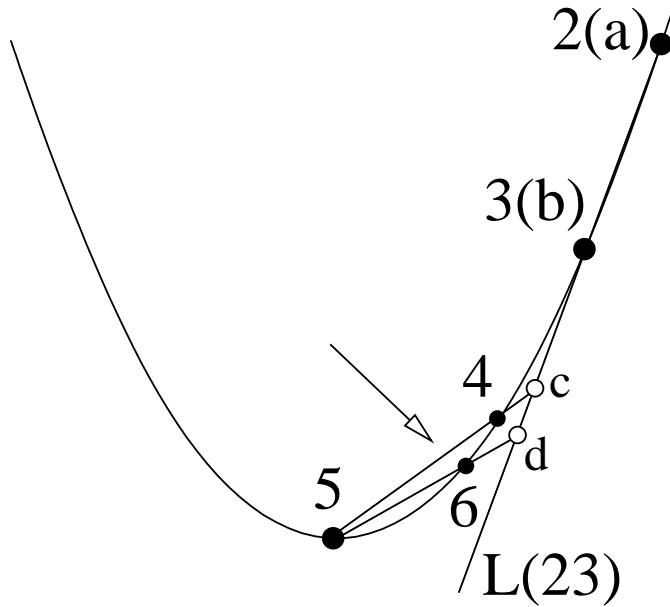


Figure 6.2: The relevant points.

6.5 The Second Estimate

Now we consider the case $k = 7$ of the Variation Lemma.

Lemma 6.7 $L_m(67) \rightarrow L(67)$.

Proof: From our analysis of the case $k = 6$, we get

$$\|V_m(6) - V(4)\| \sim \epsilon_m; \quad L_m(64) \rightarrow L(64); \quad L_m(63) \rightarrow L(63). \quad (49)$$

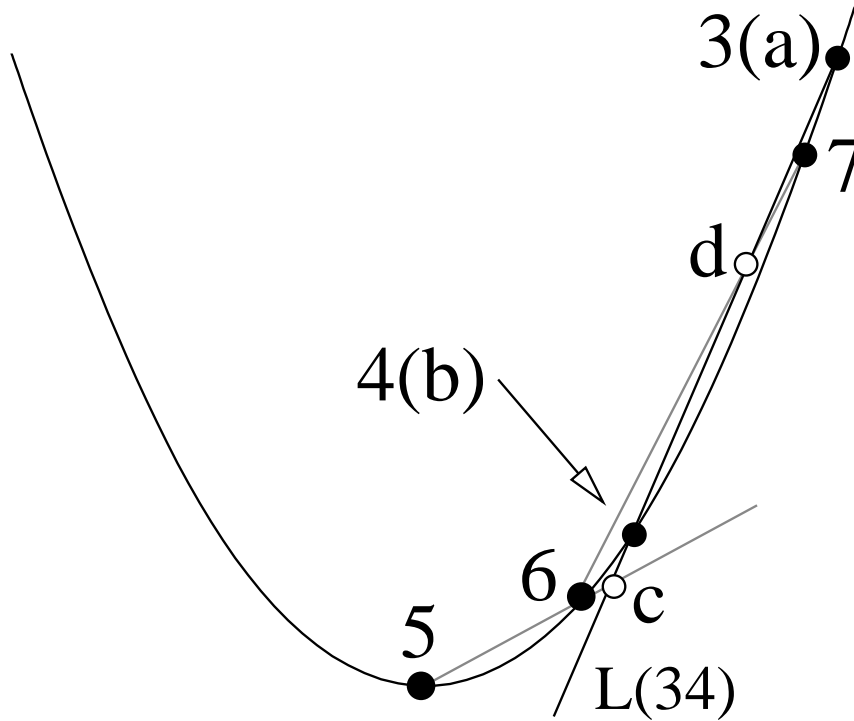


Figure 6.3: The relevant points

Suppose that $L_m(67) \not\rightarrow L(67)$. Passing to a subsequence, we can assume

$$\text{angle}(L_m(67), L_m(63)) > C$$

But, referring to Figure 6.3, this big angle combines with Equation 49 to give

$$\|d - c\| \sim \epsilon_m.$$

But then $x_5(P_m)$ does not converge to 1. This contradicts Equation 37. ♠

Lemma 6.8 $L_m(57) \rightarrow L(57)$.

Proof: It follows from our analysis in the case $k = 6$ that

$$\text{angle}\left(L_m(45), L_m(56)\right) \sim \epsilon_m. \quad (50)$$

The first of these lines is independent of m . Suppose that $L_m(57) \not\rightarrow L(57)$. Passing to a subsequence, we can assume

$$\text{angle}\left(L_m(57), L_m(53)\right) > C$$

But then

$$|1 - z_5(P_m)| > C\epsilon_m,$$

contradicting Lemma 6.6. ♠

Since the limiting lines have different slopes, and intersect only at $V(7)$, these two results combine to say that $V_m(7) \rightarrow V(7)$.

6.6 A Technical Lemma

Let $P'_m = P^{\epsilon_m}$. The twisted polygon P_m is the twist of P'_m , so to speak. Let $V'_m(k)$ denote the k th vertex of P'_m . We have $V'_m(k) = V_m(k) = V(k)$ for $k = 2, 3, 4, 5$. By our normalization, these vertices do not change with the parameters. The difficulty in the following lemma is that both the numerator and denominator tend to 0.

Lemma 6.9 *As $m \rightarrow \infty$ we have*

$$\frac{\|V_m(6) - V'_m(6)\|}{\|V(4) - V'_m(6)\|} \rightarrow 0. \quad (51)$$

Proof: Our proof refers to Figure 6.4, a copy of Figure 5.2. By the scaling rule, we have $z_4(P_m) = z_4(P'_m)$. Also the points $V_m(k)$ and $V'_m(k)$ do not depend on m for $k = 2, 3, 4, 5$. Hence, neither do the lines determined by these points. This means that the same line $\mathbf{L} = L_m(46) = L'_m(46)$ contains both $V_m(6)$ and $V'_m(6)$.

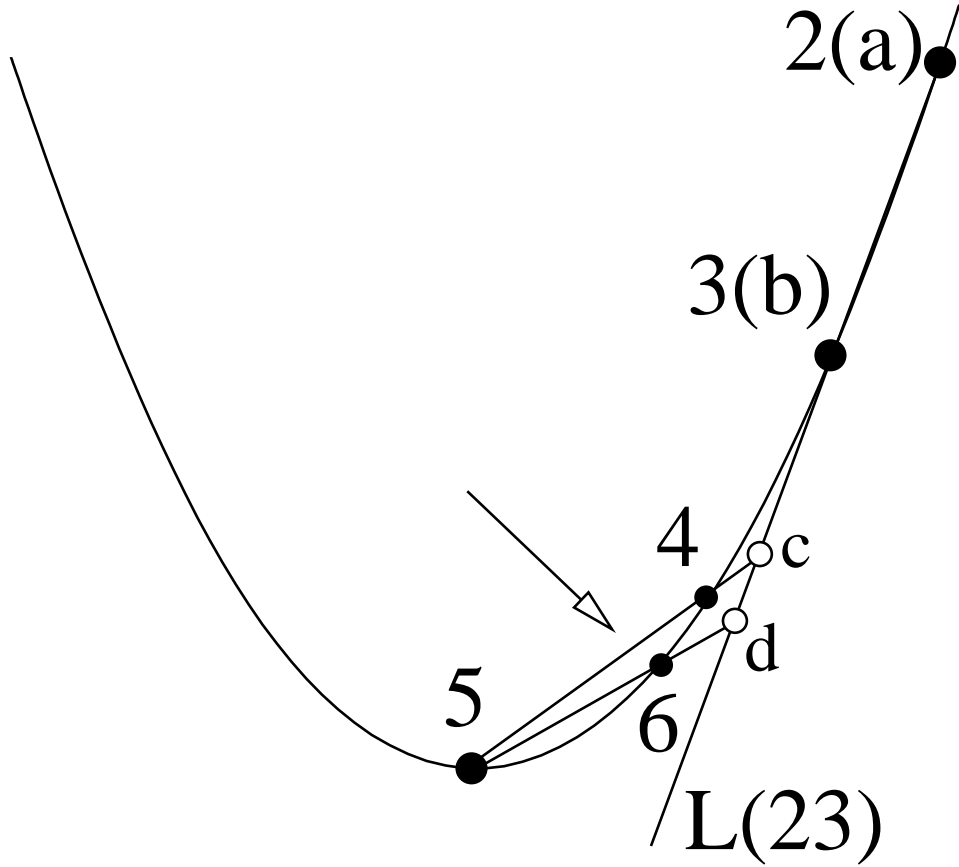


Figure 6.4: Estimating x_4 .

In Figure 6.4, the points a, b, c do not depend on m . Hence, there is a constant K such that $x_4(P_m) = K\|c - d_m\|$ and $x_4(P'_m) = K\|c - d'_m\|$. But the ratio of these quantities, namely t_m , tends to 1 as $m \rightarrow \infty$. Therefore,

$$\frac{\|c - d_m\|}{\|c - d'_m\|} \rightarrow 1 \quad \frac{\|d'_m - d_m\|}{\|c - d'_m\|} \rightarrow 0. \quad (52)$$

The first equation in Equation 52 implies the second. Geometrically, the lines $L'_m(56)$ and $L_m(56)$ make an angle which is vanishingly small with respect to the angle between either of these lines and $L(45)$. Also, all of these lines make a definite angle with $L(23)$ and \mathbf{L} . These facts combine with Equation 52 to establish this lemma. ♠

6.7 The Third Estimate

Now we consider the case $k = 8$ of the Variation Lemma.

Lemma 6.10 $L_m(68) \rightarrow L(68)$.

Proof: Note that $z_6(P)$ exists and lies in $\mathbf{C} - \{0, 1\}$, because the lines $L(6k)$ are distinct for $k = 4, 5, 7, 8$. (We interpret $L(64)$ as the line tangent to the parabola at $V_4(P) = V_6(P)$.) Moreover, if we fix $t = 1$ and let $\epsilon_m \rightarrow 0$, these lines all converge.

Now we consider what happens when t is allowed to vary. We have

$$z_6(P_m) = z_6(P_{t_m}^{\epsilon_m}) = z_6(P^{\epsilon_m}) \rightarrow z_6(P). \quad (53)$$

From previous work, we have

$$L_m(6k) \rightarrow L(6k); \quad k = 4, 5, 7. \quad (54)$$

This forces $S_m(68) \rightarrow S(68)$. But we already know $V_m(6) \rightarrow V(6)$. Hence $L_m(68) \rightarrow L(68)$. ♠

Now we show that $L_m(78) \rightarrow L(78)$. Once we know this, the same argument as in Estimate 2 shows that the Variation Lemma holds for $k = 8$.

Our proof that $L_m(78) \rightarrow L(78)$ is delicate, because many of the quantities involved are converging to 0, and the result turns on the rates of convergence. Lemma 6.9 is the main technical tool. We also make some auxiliary observations here, before starting the proof, which will help with the argument.

1. $\text{dist}(V'_m(6), L(45)) \sim \|V(4) - V'_m(6)\|$.
2. $V'_m(6) \rightarrow V(4) = V(6)$.
3. $V'_m(7)$ and $V_m(7)$ both converge to $V(7)$.
4. The line $L(47) = L(67)$ is not parallel to the line $L(45) = L(65)$.

All these properties come from our model, except the third one, which comes from the Variation Lemma for $k = 7$. See Figure 6.5 below. We call these properties together *the convergence properties*. Now we prove our final result.

Lemma 6.11 $L_m(78) \rightarrow L(78)$.

Proof: What we will do is produce 2 distinct points on $L_m(78)$ which converge to 2 distinct points on $L(78)$.

We consider the cross ratio $x_6(P_m)$. This is the cross ratio of the 4 points a, b, c, d shown in Figure 6.5. In Figure 6.5, the points $a = a_m$ and $b = b_m$ are independent of m . The points c_m and d_m depend on m . Suppose we could show that $d_m \rightarrow d$. Then, since the Variation Lemma holds for index 7, we would have two points on $L_m(78)$, namely $V_m(7)$ and d_m , converging to the distinct points $V(7)$ and d on $L(78)$. This suffices, as we already mentioned. So, to finish the proof, we just have to show that $d_m \rightarrow d$. This is what we do.

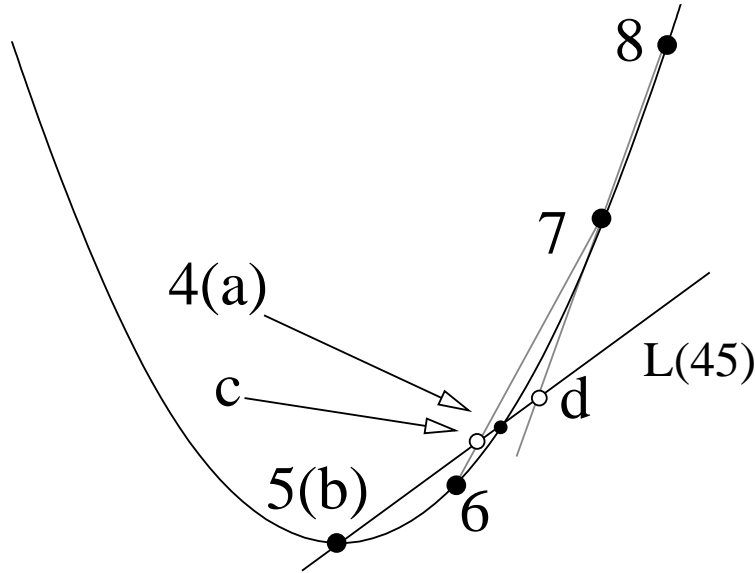


Figure 6.5: The relevant points

It follows from the convergence properties that $c_m \rightarrow c = a$. Since d_m lies on the line $\overline{bc_m}$, it suffices to prove that

$$\rho_m := \frac{\|d_m - b\|}{\|d_m - c_m\|} \rightarrow \frac{\|d - b\|}{\|d - c\|}. \quad (55)$$

We introduce the auxilliary points

$$c'_m = c(P^{\epsilon_m}); \quad d'_m = d(P^{\epsilon_m}). \quad (56)$$

That is, we reconsider the picture when t_m is replaced by 1. Since $d'_m \rightarrow d$, it suffices to prove that

$$\frac{\|c_m - d_m\| \|b - d'_m\|}{\|c'_m - d'_m\| \|b - d_m\|} = \frac{\rho'_m}{\rho_m} \rightarrow 1. \quad (57)$$

Since $t_m \rightarrow 1$, we have

$$\frac{\|a - b\| \|c_m - d_m\| \|a - c'_m\| \|b - d'_m\|}{\|a - b\| \|c'_m - d'_m\| \|a - c_m\| \|b - d_m\|} = \frac{x_4(P^{\epsilon_m})}{x_4(P_m)} \rightarrow 1. \quad (58)$$

In view of Equation 58, Equation 57 is equivalent to either of these limits:

$$\frac{\|a - c_m\|}{\|a - c'_m\|} \rightarrow 1, \quad \frac{\|c_m - c'_m\|}{\|a - c'_m\|} \rightarrow 0. \quad (59)$$

We will establish the second limit.

Looking at our model, we see that

$$\|a - c'_m\| \sim \|V(4) - V'_m(6)\|. \quad (60)$$

So, it suffices to prove

$$\frac{\|c_m - c'_m\|}{\|V(4) - V'_m(6)\|} \rightarrow 0. \quad (61)$$

We introduce the auxilliary point

$$c''_m = \overline{V_m(7) \cap V'_m(6)} \cap L(45). \quad (62)$$

For comparison,

$$c'_m = \overline{V'_m(7) \cap V'_m(6)} \cap L(45), \quad c_m = \overline{V_m(7) \cap V_m(6)} \cap L(45). \quad (63)$$

c'_m and c''_m only differ in that we are using different versions of $V_m(7)$ to define them. It follows from the convergence properties listed above that

$$\frac{\|c'_m - c''_m\|}{\|V(4) - V'_m(6)\|} \rightarrow 0. \quad (64)$$

c_m and c''_m only differ in that we are using different versions of $V_m(6)$ to define them. Combining Lemma 6.9 with the convergence properties above, we get

$$\frac{\|c_m - c''_m\|}{\|V(4) - V'_m(6)\|} \rightarrow 0. \quad (65)$$

Equation 61 follows from Equations 64 and 65. This completes our proof ♠

7 References

[DiFK], R. Kedem and P. DiFrancesco, *T-Systems with boundaries from network solutions*, Electron. J. Combin. 20 (2013) no. 1, Paper 3, 62 pp.

[FM] V. Fock, A. Marshakov, *Integrable systems, clusters, dimers and loop groups*, preprint (2013) arXiv:1401.1606

[GK] A. B. Goncharov and R. Kenyon, *Dimers and Cluster Integrable Systems*, preprint, arXiv 1107.5588 (2011)

[GSTV] M. Gekhtman, M. Shapiro, S. Tabachnikov, A. Vainshtein, *Higher pentagram maps, weighted directed networks, and cluster dynamics*, Electron. Res. Announc. Math. Sci. **19** (2012) 1–17

[Gli1] M. Glick, *The pentagram map and Y-patterns*, Adv. Math. **227** (2012) 1019–1045

[Gli2] M. Glick, *The pentagram map and Y-patterns*, 23rd Int. Conf. on Formal Power Series and Alg. Combinatorics (FPSAC 2011), 399–410

[KS1] B. Khesin, F. Soloviev *Integrability of higher pentagram maps*, Mathem. Annalen. **357**, no. 3 (2013) 1005–1047

[KS2] B. Khesin, F. Soloviev *The Pentagram Map in Higher Dimensions and KdV Flows*, Electron. Res. Announc. Math. Sci. **19** (2012), 86–96

[KS3] B. Khesin, F. Soloviev *The Geometry of Dented Pentagram Maps*. arXiv:1308.5363 (2013)

[MB1] G. Mari Beffa, *On Generalizations of the Pentagram Map: Discretizations of AGD Flows*, J. Nonlinear Sci. **23** no. 2 (2013) 303–334

[MB2] G. Mari Beffa, *On integrable generalizations of the pentagram map* arXiv:1303.4295 (2013)

[Mot] Th. Motzkin, *The pentagon in the projective plane, with a comment on Napier's rule*, Bull. Amer. Math. Soc. **52** (1945) 985–989.

[**OST**] V. Ovsienko, R. Schwartz, S. Tabachnikov, *Quasiperiodic motion for the pentagram map*, Electron. Res. Announc. Math. Sci. **16** (2009) 1–8.

[**OST1**] V. Ovsienko, R. Schwartz, S. Tabachnikov, *The pentagram map: A discrete integrable system*, Comm. Math. Phys. **299** (2010) 409–446.

[**OST2**] V. Ovsienko, R. Schwartz, S. Tabachnikov, *Liouville-Arnold integrability of the pentagram map on closed polygons*, Duke Math J., Vol. 162 (2013), 2815-2853

[**Sch1**] R. Schwartz, *The pentagram map*, Experiment. Math. **1** (1992) 71–81.

[**Sch2**] R. Schwartz, *The pentagram map is recurrent*, Experiment. Math. **10** (2001) 519–528.

[**Sch3**] R. Schwartz, *Discrete monodromy, pentagrams, and the method of condensation*, J. of Fixed Point Theory and Appl. **3** (2008) 379–409

[**Sch4**] R. Schwartz, *The Poncelet Grid*, Adv. in Geometry, **7** (2006) 157-175

[**Sol**] F. Soloviev *Integrability of the Pentagram Map*, Duke Math J., Vol. 162 (2013) 2815-2853

[**ST**] R. Schwartz, S. Tabachnikov, *Elementary surprises in projective geometry*, Math. Intelligencer **32** (2010) 31–34.